HHS Public Access

Author manuscript

Cell Rep. Author manuscript; available in PMC 2017 August 31.

Published in final edited form as:

Cell Rep. 2017 August 29; 20(9): 2169–2183. doi:10.1016/j.celrep.2017.07.082.

The Deacetylase HDAC6 Mediates Endogenous Neuritic Tau Pathology

Jui-Heng Tseng[1,2], **Ling Xie**[3], **Sheng Song**[4], **Youmei Xie**[1], **Lauren Allen**[1], **Deepa Ajit**[1,2], **Jau-Shyong Hong**[4], **Xian Chen**[3], **Rick B. Meeker**[1], and **Todd J. Cohen**[1,2,5,*]

[1]Department of Neurology, University of North Carolina, Chapel Hill, NC 27599, USA

[2]UNC Neuroscience Center, University of North Carolina, Chapel Hill, NC 27599, USA

[3]Department of Biochemistry and Biophysics, University of North Carolina, Chapel Hill, NC 27599, USA

[4]Neuropharmacology Section, Neurobiology Laboratory, National Institute of Environmental Health Sciences, Research Triangle Park, NC 27709, USA

Summary

The initiating events that promote tau mislocalization and pathology in Alzheimer's disease (AD) are not well defined, due partly to the lack of endogenous models that recapitulate tau dysfunction. We exposed wild-type neurons to a neuroinflammatory trigger and examined the impact on endogenous tau. We found that tau re-localized and accumulated within pathological neuritic foci, or beads, comprised of mostly hypo-phosphorylated, acetylated, and oligomeric tau. These structures were detected in aged wild-type mice and were enhanced in response to neuroinflammation *in vivo*, highlighting a previously undescribed endogenous age-related tau pathology. Strikingly, deletion or inhibition of the cytoplasmic shuttling factor HDAC6 suppressed neuritic tau bead formation in neurons and mice. Using mass spectrometry-based profiling, we identified a single neuroinflammatory factor, the metalloproteinase MMP-9, as a mediator of neuritic tau beading. Thus, our study uncovers a link between neuroinflammation and neuritic tau beading as a potential early-stage pathogenic mechanism in AD.

[*]Correspondence: toddcohen@neurology.unc.edu (T.J.C), Department of Neurology, UNC Neuroscience Center, University of North Carolina at Chapel Hill, 115 Mason Farm Road, NRB 6109A, CB #7250, Chapel Hill, NC 27599, USA, Tel.: 919-966-3759.
[5]Lead Contact

Author Contributions

J.H.T. performed most of the neuron-based experiments as well as the mouse/human AD brain histology. L.X. performed mass spectrometry and secretome analysis. S.S. performed brain histology on saline and LPS-injected mice, which was supervised by J.S.H. Y.X. performed brain histology and immunoblotting. L.A. assisted with live calcium imaging and quantification of tau-1_{IR} clusters. D.A performed immunohistochemical staining of aged mouse brains. J.S.H developed and supervised experiments involving the *in vivo* LPS mouse model. X.C. supervised the mass spectrometry and proteomics analysis. R.B.M. performed and supervised the analysis of neurons, hMDM, and microglia cultures, as well as brain histology of young and aged wild-type mice. T.J.C. supervised this study and wrote the manuscript with input from all authors.

Conflict of interest

The authors declare no competing conflicts of interests.

Graphical Abstract

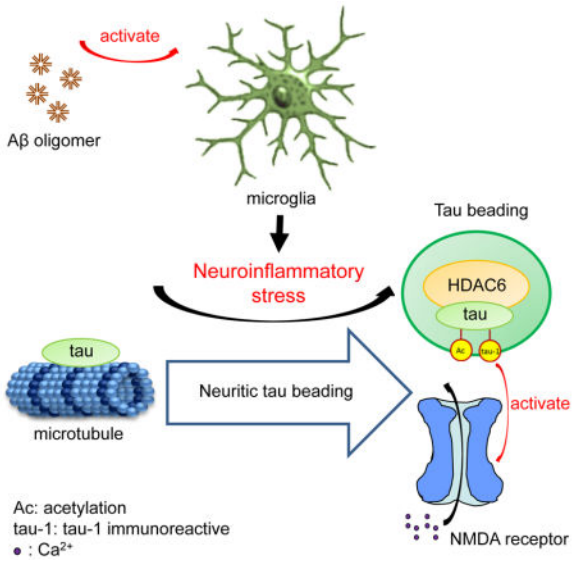

Keywords

Alzheimer's; deacetylase; excitotoxic; neuroinflammatory; tau

Introduction

Tau proteins, which comprise six distinct tau isoforms in the brain, normally act to bind and stabilize neuronal microtubules (MTs) (Andreadis, et al. 1992; Goedert, et al. 1989). The regulation of tau binding to MTs is dependent on serine/threonine phosphorylation predominantly in the proline-rich region and also by lysine acetylation directly within the MT-binding repeat region (MTBR). These two post-translational tau modifications act in concert to decrease tau-MT binding affinity (Biernat, et al. 1993; Bramblett, et al. 1993; Drechsel, et al. 1992). While tau hyper-phosphorylation has been extensively characterized in association with neurofibrillary tangle (NFT) pathology in Alzheimer's disease (AD), the role for tau acetylation in neurons is not fully understood. However, recent studies indicate that acetylated tau alone is sufficient to promote tau aggregation, synapse degeneration, and cognitive deficits in tauopathies (Min, et al. 2015; Tracy, et al. 2016).

Site-specific tau acetylation has been identified spanning the MTBR domain (Morris, et al. 2015). Recent studies showed that acetylation occurs within and adjacent to the MTBR including K174, K274, K281 that can lead to tau-induced toxicity (Min, et al. 2015; Tracy, et al. 2016). Our previous studies showed a striking accumulation of acetylated tau at residue K280 (located in the 2nd MTBR) in AD patients and a wide spectrum of other human 4-repeat (4R) tauopathies including corticobasal degeneration (CBD) and progressive supranuclear palsy (PSP) (Cohen, et al. 2011). While tau K280 acetylation is an excellent marker of AD progression that correlates with thioflavin-positive mature neurofibrillary tangles (NFTs), we detected limited tau acetylation in wild-type cultured neurons or control human brain tissue, suggesting tau acetylation may selectively accumulate in response to

specific neurotoxic cues that remain to be identified (Cohen, et al. 2011; Irwin, et al. 2012). Most tau toxicity studies rely on tau over-expression paradigms rather than modeling endogenous tau pathology. A better understanding of the initiating events that trigger early-stage endogenous tau pathogenesis will provide new avenues to prevent dysfunction in AD and related tauopathies.

Some of the very earliest neuronal dysfunction in AD includes calcium dysregulation and the development of focal neuritic beads (also known as swellings or varicosities) within axons and dendrites (Falzone and Stokin 2012; Hall, et al. 2000; Pike, et al. 1992; Sanchez-Varo, et al. 2012; Stokin, et al. 2005; Takeuchi, et al. 2005). While Aβ plaques and NFTs are the most well-established hallmark features of AD, focal beading is also a prominent yet poorly understood marker of neuronal damage that occurs in a range of neurodegenerative diseases including AD (Xiao, et al. 2011), Parkinson's disease (PD) (Tagliaferro and Burke 2016), amyotrophic lateral sclerosis (ALS) (Delisle and Carpenter 1984; Okamoto, et al. 1990), traumatic brain injury (Johnson, et al. 2013), and normal brain aging (Geula, et al. 2008). Neuritic beading is also induced by neurotoxic stimuli such as glutamate (Hosie, et al. 2012; Kim, et al. 2010), nitric oxide (NO) (He, et al. 2002), hypoxia (Scott, et al. 2002), oxidative stress (Roediger and Armati 2003), and membrane shearing (Kilinc, et al. 2009).

Prior studies indicate that neuritic beading correlates with excitotoxicity and degenerating synapses in AD (Greenwood, et al. 2007; Takeuchi, et al. 2005; Tan, et al. 2007). For example, neuritic beading is suppressed by pharmacological inhibition of NMDA receptors (NRs) (e.g. MK801 or AP5) or by intracellular calcium chelators (e.g. EDTA) (Kim, et al. 2010; Takeuchi, et al. 2005), supporting an NR-mediated process. While a functional role for tau in neuritic bead formation has not been characterized, mislocalized tau was shown to mediate NR activation through dendritic recruitment of the kinase Fyn (Ittner, et al. 2010; Roberson, et al. 2011). Tau-Fyn mislocalization to the dendritic compartment facilitates NR-subunit phosphorylation (Ittner, et al. 2010; Zempel, et al. 2010). Indeed, reducing tau or Fyn levels alleviated hyper-excitability and neurotoxicity in models of AD or traumatic brain injury (Cheng, et al. 2014; Kaufman, et al. 2015; Roberson, et al. 2011; Roberson, et al. 2007). Thus, two seemingly distinct pathological phenomenon, neuritic bead formation and tau mislocalization, are implicated as triggers for excitotoxicity in AD. Whether these two events are coordinated to mediate neuronal dysfunction is unknown.

Here, we used Aβ oligomer-challenged macrophages and microglia to generate conditioned media containing neuroinflammatory factors in order to assess the downstream effects on endogenous neuronal tau. Surprisingly, we found that tau re-localized to neuritic bead-like foci that showed features of AD pathology. Inhibiting or depleting the tau-associated deacetylase HDAC6 suppressed tau mislocalization and neuritic bead formation. Overall, our study describes a mechanism that connects neuroinflammation to focal tau accumulation as a potential early-stage tau pathology that emerges prior to the development of overt NFTs.

Results

Aβ-oligomer induced neuroinflammatory stress promotes neuritic tau-immunoreactive beading

We considered the possibility that neuroinflammation present in the brains of tau transgenic (PS19) mice and human AD brain, but not in isolated neuronal cultures, could potentially explain the striking tau mislocalization and acetylation patterns observed *in vivo*. Thus, we examined Aβ oligomer-induced neuroinflammation as a plausible mediator of endogenous tau dysfunction. Synthetic $A\beta_{1–42}$ oligomers were generated and confirmed by three independent methods: the appearance of multimeric Aβ species, A11 oligomer immunoreactivity, and dynamic light scattering (DLS) (Figure S1). Human monocyte-derived macrophages (referred to as hMDM) were challenged with Aβ oligomers and cell morphology was monitored. We used the lowest non-toxic Aβ oligomer concentration (1 μM) capable of activating immune cells *in vitro* (Dhawan, et al. 2012). Aβ oligomer stimulation increased the appearance of podosome-bearing cells compared to ruffled and non-specialized cells. Such a conversion was previously shown to correlate with secretion of neurotoxic factors (Williams, et al. 2015). Quantification of this morphology transformation showed a significant increase in podosome containing cells after 24 hr Aβ oligomer stimulation (Figure S1). Thus, in an analogous manner to HIV virion particles (Meeker, et al. 2016), Aβ oligomers were sufficient to generate conditioned media (hereafter referred to as Aβ-CM) that was subsequently evaluated for its pathogenic effects on cultured neurons.

Primary cortical neurons were exposed to Aβ-CM and tau localization was assessed using a panel of well-characterized tau antibodies (Figure 1A and Table S1). Surprisingly, Aβ-CM derived from either hMDM or microglia (the latter designated as mAβ-CM) induced the accumulation of tau within distinct neuritic beads that were detected with the dephosphorylation-specific tau-1 antibody (Figure 1A), which were not detected in tau KO neurons (Figure S2). We note that conditioned media generated by other inflammatory cues (e.g. HIV virion particles) can also induce neuritic tau beading (Figure S3). We refer to these structures as tau-1 immunoreactive (tau-1_{IR}) foci or beads. Quantification of tau-1_{IR} beading showed a significant ~ 12-fold induction in response to Aβ-CM (Figure 1B). Endogenous mouse tau detected with T49, K9JA, or tau-5 antibodies was also localized to distinct neuritic foci, although the tau-1 antibody appears to have slightly higher affinity and detection sensitivity for these structures. In contrast, we observed limited neuritic immunoreactivity with the phospho-tau AT8 (S202/T205) antibody, which is commonly used to mark tau pathology in AD. To confirm that the observed beading is due to Aβ-CM and not residual Aβ oligomers present in the conditioned media, Aβ oligomers (AβO, 1 μM) were added directly to neurons (Figure 1A and 1B), which did not induce significant morphological changes. These results suggest that secreted neuroinflammatory factors produced in the Aβ-CM are responsible for tau re-localization and accumulation within neuritic beads.

Neuritic tau beads are comprised of site-specific phosphorylated, acetylated, and oligomeric tau

We next analyzed additional acetylated and phosphorylated tau epitopes known to accumulate in AD brain. While tau K280 acetylation is not normally detected in wild-type neurons, tau beads were strikingly immunoreactive with ac-K280 (Figure 1C), a disease-specific marker of tauopathy (Cohen, et al. 2011). Despite the fact that AT8 was negative, neuritic beads were phosphorylated at an adjacent epitope (S199) in the proline-rich region (Figure 1D) and also within the MTBR (S262), a preferred MARK2 phosphorylation site (Figure 1E) (Drewes, et al. 1997). Further supporting MARK2 involvement, active MARK2 detected with a phospho-MARK antibody (residue T208) was present within tau beads, albeit less abundant compared to its phospho-tau S262 target site (Figure 1F). Both K280 acetylation and S262 phosphorylation have been implicated in dissociation of tau from MTs (Cohen, et al. 2011; Schwalbe, et al. 2013), suggesting tau beading coincides with loss of normal tau-MT binding. We next examined oligomeric tau, an indicator of early-stage tau pathology (Lasagna-Reeves, et al. 2012), using the T22 antibody and found that it was highly enriched within neuritic tau-1_{IR} beads (Figure 1G, see quantification in Figure 1H).

We further analyzed a panel of dendritic markers implicated in aberrant tau-mediated neuronal hyper-excitability. Neuritic tau beads co-localized with the dendritic marker MAP2, the tau kinase Fyn implicated in tau recruitment to the dendritic compartment, as well as NR1, a major NMDA receptor subunit that is subject to phosphorylation-dependent activation and excitotoxicity (Ittner, et al. 2010; Roberson, et al. 2011) (Figure S4). We also examined the localization of other factors involved in protein quality control including autophagy and ubiquitin-proteasome system (UPS) components that regulate tau processing and triage. The deacetylase HDAC6, an adaptor protein that detects and shuttles misfolded proteins (Kawaguchi, et al. 2003) and also binds and deacetylates tau (Cohen, et al. 2011; Ding, et al. 2008; Perez, et al. 2009), strongly localized to most tau-1_{IR} beads (Figure 2A). Similarly, the E3 ligase CHIP and the 20S proteasome, implicated in tau processing, were localized to neuritic beads, while autophagosomal markers such as LC3 were not prominently detected within these structures (Figure S4). Overall, our analysis indicates that tau beads recruit a variety of axonal and dendritic factors known to interact with and process tau.

HDAC6 depletion or inhibition suppresses neuritic bead formation

We sought to identify a mechanism by which neuritic tau beads form in vulnerable neurons. Given the robust recruitment of HDAC6 to tau-1_{IR} beads, we asked whether manipulating HDAC6 levels or activity would alter tau beading in Aβ-CM treated neurons. We used HDAC6 KO neurons (Figure 2B) as well as pharmacological exposure of wild-type neurons to tubastatin A (TBST), a selective HDAC6 inhibitor (Figure S5). Remarkably, elimination of HDAC6 showed nearly a complete loss of neuritic tau beads (Figure 2B) as well as reduced focal recruitment of degradative and synaptic components to bead-like structures (Figure 2C–E). Overall there was a ~ 90% reduction in tau beading in HDAC6 KO neurons (Figure 2F), supporting HDAC6-dependent neuritic bead formation. A similarly dramatic suppression of beading was observed with TBST treatment (Figure 2F and Figure S5).

To investigate the physiological consequences of tau beading, we assessed the viability of neurons challenged with Aβ-CM in the presence or absence of TBST. Using independent survival assays that monitor neuronal death or metabolic function, we found that TBST partially alleviated only the neuronal death phenotype as assessed by LDH assay, but did not significantly alter the reduction in metabolic activity assessed by MTT assays (Figure 2G), suggesting a neuroprotective effect that is independent of mitochondrial function. Surprisingly, mild neuroprotection occurred despite the fact that tau acetylation levels were increased in neurons exposed to TBST (Figure S5).

Since neuronal death in AD is linked to excitotoxicity, we asked whether tau-1_{IR} bead formation is associated with intracellular calcium increases that occur following NR activation. Live calcium imaging was performed in Aβ-CM challenged neurons in the absence or presence of TBST to suppress tau-1_{IR} beading (Figure 3). Excitotoxicity is associated with delayed and sustained elevation of intracellular calcium, and we therefore monitored both the early acute and delayed calcium changes occurring over a ~ 60 min period following exposure to Aβ-CM. Aβ-CM induced an acute calcium rise in the neuronal cytoplasm followed by a gradual delayed calcium increase (Figure 3A). Notably, discrete foci of calcium accumulation were seen in axonal and dendritic processes, which gave rise to neuritic beads (Figure 3A, see white arrowheads at 10, 30, and 60 min time-points). Conditioned media generated from Aβ-challenged hMDM (Aβ-CM), Aβ-challenged microglia (mAβ-CM), or even HIV virion-challenged hMDM (HIV-CM) induced comparable calcium dysregulation in neurons (Figure 3B and Figure S3). HDAC6 KO or TBST treatment dramatically reduced calcium influx throughout the incubation period by ~ 4–5 fold, including at the endpoint of the delayed calcium phase (Figure 3B and 3C). The calcium influx and beading were also strongly inhibited by the NMDA receptor antagonist AP5, suggesting that tau-1_{IR} beads represent active sites of NMDA-receptor driven calcium influx. In contrast, inhibition of MARK2 (also localized to neuritic beads, Figure 1F) using MARK inhibitor 39621 did not affect calcium influx (Figure 3C).

We next assessed the impact of Aβ-CM on tau by immunoblotting using a panel of tau antibodies (Figure S5). Total tau levels were not appreciably altered in Aβ-CM challenged neurons, consistent with tau mislocalization as a key pathological indicator, as opposed to changes in overall tau stability. Tau hypo-phosphorylation was observed at most phospho-tau epitopes including AT180 (T231) and AT270 (T181) in response to Aβ-CM, and this effect that was partially restored by inhibition of neuritic beading with either TBST or AP5. Furthermore, levels of acetylated tubulin, a marker of stable microtubules, were also restored by TBST. Thus, we conclude that neuroinflammatory factors stimulate HDAC6-dependent tau re-localization, tau hypo-phosphorylation at most common pathological tau epitopes, and the formation of axonal and dendritic tau-1_{IR} beads.

In vivo neuritic tau-1_{IR} pathology in mouse and human brain

We considered whether the neuritic tau-1_{IR} species detected above could be recapitulated *in vivo*. Although endogenous tau pathology is not typically detectable in normal wild-type mice, we asked whether tau-1_{IR} pathology might accumulate as a consequence of aging, the major risk factor for AD. In contrast to young mice that showed faint diffuse axonal tau-1

staining patterns throughout the brain, aged 27 month old mice showed a striking accumulation of tau-1_{IR} foci that were concentrated as distinct patches or clusters throughout the hippocampus, particularly in CA1, and distributed more selectively throughout cortical brain regions (Figure 4A). Tau-1 immunoreactive clusters gradually accumulated with age, as assessed by immunoblotting (Figure 4B), immunofluorescence (Figure 4C), and immunohistochemistry (Figure 4D). These structures became more readily detectable starting around 12 months old (see quantification in Figure 4E).

We examined whether a neuroinflammatory challenge could modulate tau-1 immunoreactivity *in vivo* in a manner similar to our observations *in vitro* using Aβ-CM (Figure 1). We employed a lipopolysaccharide (LPS) injection paradigm in which a single LPS dose (5 mg/kg) given to young 3-month old mice was sufficient to induce chronic long-term neuroinflammation up to 10 months post LPS injection (Qin, et al. 2007). We observed a significant increase in tau-1_{IR} pathology in LPS-stimulated mice compared to age-matched saline injected controls (Figure 4F, see quantification in Figure 4G). Thus, tau-1_{IR} pathology accumulates as a general feature of normal brain aging that can be significantly accelerated by neuroinflammatory cues.

To examine the nature of tau-1_{IR} clusters *in vivo*, double-labeling of aged mouse brain sections was performed with tau-1 and either ac-K280, T22, or MAP2 antibodies, all of which detected neuritic tau beads *in vitro*. Similarly, *in vivo* tau-1_{IR} clusters were ac-K280-positive, strongly T22-immunoreactive, and also partially accumulated in the dendritic compartment as assessed by co-localization with MAP2 (Figure 5A). We note that these structures are labeled with the same antibodies that detected tau-1_{IR} foci *in vitro*, and are not AT8-immunoreactive or detectable by standard Thioflavin-S staining (Figure S6). Tau-1_{IR} pathology in mouse brain therefore appears to represent a biochemically distinct age-related tau species. Similar to HDAC6-mediated tau beading *in vitro* (Figure 2), tau-1_{IR} clusters were suppressed in the brains of HDAC6 KO mice (Figure 5B, see quantification in Figure 5C). The reduced tau-1_{IR} pathology could potentially explain the restored cognitive function observed with HDAC6 depletion or inhibition (Govindarajan, et al. 2013; Selenica, et al. 2014; Zhang, et al. 2014).

Hyper-phosphorylated tau (e.g. AT8 immunoreactive tau) is commonly used to monitor tau pathology in human AD brain. In contrast, dephosphorylated tau-1_{IR} pathology, an epitope that overlaps with AT8, has not been well studied in postmortem tissue. However, since Aβ facilitated the formation of tau-1_{IR} pathology *in vitro*, we asked whether tau-1 immunoreactivity was associated with Aβ plaque pathology in AD brain. We performed double-labeling with the tau-1 antibody and Thioflavin S (ThS), the latter of which robustly marked AD neuritic plaques and thread-like tau pathology. Indeed, tau-1 immunoreactivity was clearly detected in a subset of neuritic plaques and tau inclusions in AD brain. As a control, neuritic plaques were immunoreactive with the Aβ-specific 6E10 antibody (Figure 6A).

To further confirm tau-1_{IR} pathology using biochemical methods, we performed a sequential extraction of frontal cortex from control and AD brains and analyzed soluble and insoluble tau species by immunoblotting (Figure 6B). We observed a reduction of tau-1

immunoreactivity in soluble high-salt fractions and a concomitant increase in the insoluble tangle-rich fractions (i.e. tau aggregate smearing), consistent with a conversion towards tau-1-positive pathology. While insoluble tau was also hyper-phosphorylated at other AD-relevant epitopes (e.g. S396 and S262), the phospho-tau immunoreactive banding patterns were distinct; they tended to show high and low molecular weight smearing compared to the tau-1 immunoreactive bands that migrated preferentially as monomeric tau species (Figure 6B, see asterisk). Thus, in contrast to global tau hyper-phosphorylation, dephosphorylated tau-1_{IR} pathology represents a significant pool of total pathological tau in AD brain.

Identification of neurotoxic factors linked to neuritic tau beading

Given that Aβ-CM likely consists of a mixture of secreted pro- and anti-inflammatory immune factors (Williams, et al. 2015), we sought to identify the neurotoxic factor(s) responsible for tau beading and excitotoxicity. To accomplish this, we profiled Aβ-CM using a mass spectrometry (MS)-based label-free quantitative (LFQ) approach. We identified a total of 1472 proteins, among which 817 proteins were identified with at least 2 unique peptides (Table S2). The volcano plot demonstrates significance ($-\log P$) and changes that occurred in response to Aβ oligomers (Figure 7A, displayed as $\log_2$ Aβ/untreated). Overall, 354 proteins increased and 258 proteins decreased with false-discovery-rates (FDR) < 5%. A biological function (DAVID) analysis of the 354 significantly induced hits identified factors that were enriched in immune and inflammatory responses as well as neuronal stress and apoptotic signaling pathways (Figure 7B). Further cluster analysis identified two large networks of proteins with shared functions in neuroinflammation and metabolism (Figure S7).

Among the immune factors identified in Aβ-CM, a set of matrix metalloproteinases (MMP-1, -7, and -9) were significantly altered, consistent with prior reports linking extracellular MMP activity to AD progression (Mroczko, et al. 2013; Nubling, et al. 2012; Stomrud, et al. 2010) (Figure 7A and Figure S7). Since MMP-9 levels were previously shown to increase in AD patient CSF (Stomrud, et al. 2010) as well as iPSC cell culture models of mutant tau-induced frontotemporal dementia (FTD) (Biswas, et al. 2016), we focused on MMP-9 as a candidate factor that may partially mediate the effects of Aβ-CM on tau. In contrast to most MMP family members, MMP-9 contains gelatinase activity, which is readily detected by SDS-PAGE gels supplemented with gelatin. Serial analysis of undiluted Aβ-CM detected increased gelatinase activity migrating ~ 75–100 kD (Figure 7C, top panel), indicating Aβ oligomers induced secretion of MMP-9. Moreover, direct immunoblotting of Aβ-CM with an MMP-9 specific antibody also detected active secreted MMP-9 that was not observed in the absence of Aβ oligomer stimulation (Figure 7C, bottom panel).

To test the effect of MMPs on neuritic beading, recombinant purified MMP-7 or MMP-9 were directly added to neuronal cultures. The final exposure concentration of MMP-9 (5 ng/ml) reflected known physiological MMP-9 concentrations in cerebrospinal fluid (CSF) (Ichiyama, et al. 2009). While MMP-7 had little effect on focal neuritic tau beading, MMP-9 generated tau-1_{IR} foci that were similar, although less pronounced, compared to complete Aβ-CM (Figure 7D, see quantification, right panel), suggesting MMP-9 can partially

recapitulate neuritic tau beading. To further evaluate whether MMP-9 induced calcium deregulation, live imaging was performed after recombinant MMP-9 addition to neurons, which showed an increase in the rate and intensity of calcium spikes (Figure 7E), consistent with previous reports that MMP-9 is coupled to NMDA receptor activation (Michaluk, et al. 2009). The net effect of MMP-9 was a mild accumulation of intracellular calcium that recapitulated the pattern, but not the full intensity, of the response to Aβ-CM. These data suggest that MMP-9 is sufficient to increase the vulnerability of neurons to the development of tau-1_{IR} pathology but is not solely responsible. Importantly, the MMP-9-mediated calcium increase was dependent on HDAC6 activity, as TBST significantly blunted calcium spiking by ~ 3-fold (Figure 7E, right panel). Finally, to assess the impact of MMP-9 loss of function, we incubated Aβ-CM with an MMP-9-specific inhibitor prior to calcium imaging and we observed a ~50% reduction in the acute phase calcium rise (Figure 7F). Thus, our proteomics approach uncovered a single neuroinflammatory factor, MMP-9, as one upstream mediator in the pathological cascade leading to HDAC6-dependent tau-1_{IR} beading and calcium dysregulation.

Discussion

In this study, we show that tau accumulation within neuritic beads is an endogenous neuronal response to inflammatory perturbations. In a search for mediators of neuritic bead formation, we identified the cytoplasmic deacetylase HDAC6 as a shuttling factor required for tau re-localization and calcium-mediated excitotoxicity. Further *in vivo* analysis of neuritic tau beading revealed tau-1_{IR} clusters in hippocampal and cortical regions of aged wild-type mice, supporting the accumulation of dephosphorylated tau (at the tau-1 epitope) as a plausible early-stage indicator of neuronal damage and/or vulnerability that precedes overt tangle formation. Our data indicate that acetylated, hypo-phosphorylated, and oligomeric tau accumulates at sites of focal calcium signaling in vulnerable neurons and could represent a unique tau species that is primed to undergo subsequent maturation and pathological aggregation during normal aging or the progression of AD.

Toxic Aβ induces a neuroinflammatory signature that coincides with synaptic degeneration. However, most *in vitro* neuronal models have not considered the impact of Aβ on neuroinflammation, potentially under-estimating its effects on neuronal dysfunction. Our analysis of the Aβ-induced secretome by mass spectrometry identified a subset of secreted MMPs among which MMP-9 partially recapitulated tau foci formation and calcium dysregulation. While the exact role for MMP-9 in AD pathogenesis is not fully understood, MMP-9 is implicated in neuronal activity through the activation of integrin β1 leading to phosphorylation of NMDA receptor subunits (Michaluk, et al. 2009). MMP-9 levels are up-regulated in AD and during epileptogenesis characterized by hyper-excitability and aberrant NR activity (Stomrud, et al. 2010; Wilczynski, et al. 2008). Thus, MMP-9 may be coupled to tau dysfunction similar to other excitotoxic stimuli including, for example glutamate-induced excitotoxicity, which also promotes tau hypo-phosphorylation (Davis, et al. 1995). Future studies are necessary to determine the mechanism by which extracellular MMP-9 facilitates intracellular tau mis-localization.

Tau is thought to represent ~ 0.025–0.25% total brain protein (Khatoon, et al. 1992). Thus, MT-dissociated tau requires quality-control mechanisms including proteasome and autophagy-dependent pathways to maintain proteostasis. In healthy neurons, the adaptor protein HDAC6 may bind tau and actively shuttle tau for targeted sequestration or degradation. Prior studies showed direct tau-HDAC6 binding via the tau MTBR domain (Ding, et al. 2008; Perez, et al. 2009). While HDAC6 is known to bind ubiquitinated cargo, it remains unclear whether tau-1_{IR} beads are active sites of tau triage and/or degradation. We have not observed tau ubiquitination or degradation upon treatment with Aβ-CM, despite the fact that 20S proteasomes were partially concentrated within tau-1_{IR} beads (Figure S4). Alternatively, HDAC6 deacetylates and regulates a variety of cytoplasmic factors including MTs and heat shock proteins (e.g. HSP70 and HSP90) that also directly interact with tau (Yan 2014). Therefore, HDAC6 could shuttle tau to neuritic beads indirectly via regulation of tau-associated adaptor, scaffolding, and/or structural proteins (e.g. actin and MTs). Finally, HDAC6 also shuttles to the nucleus and regulates gene transcription (Bertos, et al. 2004; Verdel, et al. 2000). Thus, it remains plausible that inhibition of HDAC6 nuclear function could partly contribute to the suppression of tau beading and excitotoxicity.

Our data suggest that under neuroinflammatory conditions HDAC6-associated complexes could become trapped within the damage-induced neuritic beads. The presence of HDAC6 initially suggested active deacetylation of tau, but in contrast, we observed increased K280-acetylated tau within beads. Therefore, we speculate that HDAC6 activity may become impaired within the dense beaded network along with other trapped vesicles and degenerated cytoskeletal components, eventually leading to increased tau acetylation, NR activation, and calcium deregulation. Increased intracellular calcium accumulation could further exacerbate neuronal toxicity via activation of downstream calcium-dependent enzymes including calpain and calcineurin, both of which have been implicated in Aβ-induced neurotoxicity (Kurbatskaya, et al. 2016; Rozkalne, et al. 2011).

Prior studies indicated that acetylated tau impairs tau-MT binding and enhances tau aggregation, toxicity, and synaptic dysfunction (Cohen, et al. 2011; Min, et al. 2015; Tracy, et al. 2016). This is supported by our previous inability to detect robust tau K280 acetylation in normal cultured neurons or control brain tissue and by our current data showing that neuroinflammatory stress may act as a trigger for the accumulation of acetylated tau (Figure 1C). We speculate that tau acetylation is pathogenic when highly concentrated within neuritic beads, which could facilitate its aggregation or perturb the cytoskeleton and associated synaptic factors including, for example, the recently described KIdney/BRAin protein (KIBRA) (Tracy, et al. 2016). By blocking HDAC6-dependent neuritic bead formation, aberrantly modified tau may not have similarly pathogenic consequences. Indeed, HDAC6 inhibition mildly induced tau acetylation (Figure S5), but this was coincident with a partial suppression of neurotoxicity (Figure 2G), suggesting enhanced tau acetylation does not necessarily correlate with neurotoxicity. A tau acetyltransferase(s) such as CBP/p300 could localize to tau beads to facilitate tau acetylation. Alternatively, local acetyl co-A accumulation within or surrounding beaded structures may be sufficient to promote tau auto-acetylation and drive tau aggregation in a localization and concentration-dependent manner (Cohen, et al. 2013).

In contrast to tau acetylation, tau hyper-phosphorylation was not prominently detected within neuritic beads, at least at several of the phospho-tau epitopes examined. This is supported by other studies showing that acetylated tau at residues K274 and K281 led to neurotoxicity and synaptic defects with little apparent hyper-phosphorylation at AD-relevant epitopes (Tracy, et al. 2016). Thus, hypo-phosphorylated yet acetylated tau could initially mark early-stage mislocalized tau followed by later stage tau hyper-phosphorylation, a step-wise modification scheme that may be required for maturation of tau aggregates into NFTs. We propose that tau-1 immunoreactive pathology could occur as an initial compensatory response in healthy, yet vulnerable neurons, which could reflect adequate PP2A activity and hence sufficient tau dephosphorylation until a certain threshold is reached. Eventually, however, tau may be further subjected to hyper-phosphorylation as a consequence of disease progression. Such a fluctuating pattern of tau phosphorylation has been observed *in vitro* (Liang, et al. 2009; LoPresti and Konat 2001). Prolonged tau-1_{IR} neuritic bead accumulation *in vitro,* beyond the timeframe allowable for cultured primary neurons, may be required for impaired PP2A function, tau re-phosphorylation, and accumulation of more mature tau aggregates.

The notion that dephosphorylated tau (at the tau-1 epitope) could be linked to tau pathology is plausible. Dephosphorylated tau is known to associate with the neuronal membrane (Arrasate, et al. 2000; Maas, et al. 2000; Pooler, et al. 2012). The close proximity of tau to the membrane could facilitate Fyn-mediated activation of NRs and increased intracellular calcium accumulation. Although tau-1 immunoreactivity is rarely assessed as a pathological marker *per se* in mouse and human tissues, we detected tau-1-positive structures as distinct clusters in aged mice, LPS-treated mice, and human AD brain, consistent with a potential role for the tau-1_{IR} species in tau pathogenesis (Figure 4). Whether the age-related tau-1_{IR} pathology identified in this study is linked to primary age-related tauopathy (PART) recently described in humans is not clear, but there are intriguing parallels, as both phenomenon show clear age-related tau deposition in the hippocampus (Crary, et al. 2014).

We have begun to elucidate the biochemical properties of tau-1_{IR} structures; they are enriched with oligomeric, acetylated, and hypo-phosphorylated tau at many AD-relevant epitopes analyzed. We have not detected robust misfolded tau epitopes (MC1 or Alz-50) or prominent amyloid conformation within tau beaded structures. Future studies could establish whether other brain pathologies including TDP-43 or Aβ facilitate endogenous tau-1_{IR} pathology, which we cannot currently exclude. Lastly, tau-1_{IR} beading *in vitro* appears to be reversible upon removal of Aβ-CM. Thus, tau-1_{IR} neuritic beads may represent a feature of neuronal vulnerability that is amenable to pharmacological intervention. Taken together, our study highlights a mechanism linking neuroinflammatory stress to HDAC6-mediated neuritic tau accumulation, which we anticipate will provide insights into normal endogenous tau regulation, excitotoxic disease mechanisms, and avenues for therapeutic interventions in AD.

Experimental Procedures

Double-label Immunofluorescence

Primary cortical neurons were grown on PDL-coated coverslips and cultured as described above and treated for indicated times. Cells were fixed in 4 % paraformaldehyde for 15 min, rinsed three times in PBS and permeabilized with 0.2 % Triton X-100 (Sigma) in PBS for 10 min. Cells were then blocked in 2% milk for 1 h, and subsequently incubated with primary antibodies of interest overnight at 4°C. Cells were washed in PBS and incubated wit Alexi-488 or 594-conjugated secondary antibody. Cells were analyzed using an Olympus IX83 Inverted Microscope. The ratio of colocalization with Tau-1 was quantified by the number of beads that contain immunoreactivity from both Tau-1 and the antibody of interest among the total number of Tau-1 positive beads, using > 5 fields, and the sampling error was calculated using S.E.M. Statistical analysis was determined using a two-tailed unpaired Student's t-test with unequal variance (significance set as P-value <0.05). All quantitative fluorescence was independently validated with a minimum of 3 different biological replicates. Primary antibodies used for immunofluorescence are listed in Table S1.

Live Calcium Imaging

Neuronal cultures were washed in HEPES-buffered artificial CSF (aCSF, concentrations in mM: NaCl 137, KCl 5, $CaCl_2$ 2.3, $MgCl_2$ 1.3, glucose 20, HEPES 10, pH 7.4) and preloaded with the calcium indicator, Fluo-4 AM using the Molecular Probes Fluo-4 NW Assay Kit (Molecular Probes/Invitrogen) at a 1:4 dilution. After 30 min, cultures were washed in aCSF and 18 mm coverslips mounted in a specialized stage for imaging (Warner Instruments). Images were captured on an Olympus IX71 inverted microscope at a temperature of 25°C which provided stable background activity for at least 2 h. TBST was added to the coverslips 3 h prior to the challenge, while MARK2 inhibitor, 39621 (Millipore), AP5, and MMP-9 inhibitor (Calbiochem) were added 30 min prior to the challenge. The cells were challenged with CM (from hMDM or mouse microglia) at a 1:4 dilution, MMP-9 (50 ng/mL) or MMP-7 (150 ng/mL). Time-lapse digital images were captured automatically by the Metamorph System (Molecular Device). Three pre-stimulation measurements were taken to establish basal levels of fluorescence at the beginning of each experiment. Acute changes in calcium were measured at 0.1 min intervals for 6 min. Delayed changes in calcium were measured at 1 min intervals for an additional 1 h. The increase in calcium intensity (free calcium) within each cell was then measured relative to the baseline measurements to correct for cell to cell differences in dye loading and intrinsic fluorescence. Control cultures were stimulated with aCSF in the same fashion to establish normal baseline calcium activity as well as any intrinsic toxic activity from the cortical neuron cultures. Spikes were evaluated compared with the control cultures. Calcium spiking frequency was calculated as the number of spikes per 100 images.

Statistical analysis

Graphpad Prism software was used for all statistical analysis. Results were pooled from a minimum of three independent experiments and presented as average ± standard error of the mean (SEM). Comparisons between two groups were analyzed using unpaired student t test. Significance was presented with *, **, or *** corresponding to p-value <0.05, p value

<0.01, or p value <0.001. Hippocampal regions with tau-1 immunoreactive (tau-1_{IR}) clusters from at least N=3 mice per age group were thresholded using Metamorph software and tau-1 intensity was plotted as the overall tau-1_{IR} density per hippocampal region. Three isolated regions were chosen at random within the areas comprising tau-1_{IR} clusters. Sections from HDAC6 KO mice that lacked tau-1_{IR} clusters were used as negative controls to account for background staining intensity.

Supplementary Material

Refer to Web version on PubMed Central for supplementary material.

Acknowledgments

Support for this work was provided by the Alzheimer's Association, grant NIRG-14-321219 (TJC), the National Center for Advancing Translational Sciences (NCATS), National Institutes of Health, grant UL1TR001111 (TJC), the American Federation for Aging Research (AFAR), grant RAG15247 (TJC), National Institutes of Health grant 1U19AI109965 (X.C.), and R01-NS083164 (R.B.M). This work was supported in part by the Intramural Research Program of the NIH/NIEHS. We thank Ms. Bhavi Vohra for assistance with human and mouse tissue analysis, Dr. Ashutosh Tripathy for assistance with dynamic light scattering (DLS), Dr. John Trojanowski (University of Pennsylvania) for providing AD patient brain samples, and Dr. Tso-Pang Yao (Duke University) for providing HDAC6 KO mice. We also thank Dr. C. Ryan Miller and the UNC Translational Pathology Laboratory (TPL) for providing fixed embedded human AD tissue, interpreting patient clinical and histology records, and providing valuable advice and support.

References

Andreadis A, Brown WM, Kosik KS. Structure and novel exons of the human tau gene. Biochemistry. 1992; 31:10626–10633. [PubMed: 1420178]

Arrasate M, Perez M, Avila J. Tau dephosphorylation at tau-1 site correlates with its association to cell membrane. Neurochem Res. 2000; 25:43–50. [PubMed: 10685603]

Bertos NR, Gilquin B, Chan GK, Yen TJ, Khochbin S, Yang XJ. Role of the tetradecapeptide repeat domain of human histone deacetylase 6 in cytoplasmic retention. The Journal of biological chemistry. 2004; 279:48246–48254. [PubMed: 15347674]

Biernat J, Gustke N, Drewes G, Mandelkow EM, Mandelkow E. Phosphorylation of Ser262 strongly reduces binding of tau to microtubules: distinction between PHF-like immunoreactivity and microtubule binding. Neuron. 1993; 11:153–163. [PubMed: 8393323]

Biswas MH, Almeida S, Lopez-Gonzalez R, Mao W, Zhang Z, Karydas A, Geschwind MD, Biernat J, Mandelkow EM, Futai K, Miller BL, Gao FB. MMP-9 and MMP-2 Contribute to Neuronal Cell Death in iPSC Models of Frontotemporal Dementia with MAPT Mutations. Stem Cell Reports. 2016; 7:316–324. [PubMed: 27594586]

Bramblett GT, Goedert M, Jakes R, Merrick SE, Trojanowski JQ, Lee VM. Abnormal tau phosphorylation at Ser396 in Alzheimer's disease recapitulates development and contributes to reduced microtubule binding. Neuron. 1993; 10:1089–1099. [PubMed: 8318230]

Cheng JS, Craft R, Yu GQ, Ho K, Wang X, Mohan G, Mangnitsky S, Ponnusamy R, Mucke L. Tau reduction diminishes spatial learning and memory deficits after mild repetitive traumatic brain injury in mice. PloS one. 2014; 9:e115765. [PubMed: 25551452]

Cohen TJ, Friedmann D, Hwang AW, Marmorstein R, Lee VM. The microtubule-associated tau protein has intrinsic acetyltransferase activity. Nat Struct Mol Biol. 2013; 20:756–762. [PubMed: 23624859]

Cohen TJ, Guo JL, Hurtado DE, Kwong LK, Mills IP, Trojanowski JQ, Lee VM. The acetylation of tau inhibits its function and promotes pathological tau aggregation. Nature communications. 2011; 2:252.

Crary JF, Trojanowski JQ, Schneider JA, Abisambra JF, Abner EL, Alafuzoff I, Arnold SE, Attems J, Beach TG, Bigio EH, Cairns NJ, Dickson DW, Gearing M, Grinberg LT, Hof PR, Hyman BT,

Jellinger K, Jicha GA, Kovacs GG, Knopman DS, Kofler J, Kukull WA, Mackenzie IR, Masliah E, McKee A, Montine TJ, Murray ME, Neltner JH, Santa-Maria I, Seeley WW, Serrano-Pozo A, Shelanski ML, Stein T, Takao M, Thal DR, Toledo JB, Troncoso JC, Vonsattel JP, White CL 3rd, Wisniewski T, Woltjer RL, Yamada M, Nelson PT. Primary age-related tauopathy (PART): a common pathology associated with human aging. Acta Neuropathol. 2014; 128:755–766. [PubMed: 25348064]

Davis DR, Brion JP, Couck AM, Gallo JM, Hanger DP, Ladhani K, Lewis C, Miller CC, Rupniak T, Smith C, et al. The phosphorylation state of the microtubule-associated protein tau as affected by glutamate, colchicine and beta-amyloid in primary rat cortical neuronal cultures. Biochem J. 1995; 309(Pt 3):941–949. [PubMed: 7639714]

Delisle MB, Carpenter S. Neurofibrillary axonal swellings and amyotrophic lateral sclerosis. J Neurol Sci. 1984; 63:241–250. [PubMed: 6538591]

Dhawan G, Floden AM, Combs CK. Amyloid-beta oligomers stimulate microglia through a tyrosine kinase dependent mechanism. Neurobiol Aging. 2012; 33:2247–2261. [PubMed: 22133278]

Ding H, Dolan PJ, Johnson GV. Histone deacetylase 6 interacts with the microtubule-associated protein tau. Journal of neurochemistry. 2008; 106:2119–2130. [PubMed: 18636984]

Drechsel DN, Hyman AA, Cobb MH, Kirschner MW. Modulation of the dynamic instability of tubulin assembly by the microtubule-associated protein tau. Molecular biology of the cell. 1992; 3:1141–1154. [PubMed: 1421571]

Drewes G, Ebneth A, Preuss U, Mandelkow EM, Mandelkow E. MARK, a novel family of protein kinases that phosphorylate microtubule-associated proteins and trigger microtubule disruption. Cell. 1997; 89:297–308. [PubMed: 9108484]

Falzone TL, Stokin GB. Imaging amyloid precursor protein in vivo: an axonal transport assay. Methods Mol Biol. 2012; 846:295–303. [PubMed: 22367820]

Geula C, Nagykery N, Nicholas A, Wu CK. Cholinergic neuronal and axonal abnormalities are present early in aging and in Alzheimer disease. J Neuropathol Exp Neurol. 2008; 67:309–318. [PubMed: 18379437]

Goedert M, Spillantini MG, Jakes R, Rutherford D, Crowther RA. Multiple isoforms of human microtubule-associated protein tau: sequences and localization in neurofibrillary tangles of Alzheimer's disease. Neuron. 1989; 3:519–526. [PubMed: 2484340]

Govindarajan N, Rao P, Burkhardt S, Sananbenesi F, Schluter OM, Bradke F, Lu J, Fischer A. Reducing HDAC6 ameliorates cognitive deficits in a mouse model for Alzheimer's disease. EMBO Mol Med. 2013; 5:52–63. [PubMed: 23184605]

Greenwood SM, Mizielinska SM, Frenguelli BG, Harvey J, Connolly CN. Mitochondrial dysfunction and dendritic beading during neuronal toxicity. The Journal of biological chemistry. 2007; 282:26235–26244. [PubMed: 17616519]

Hall GF, Chu B, Lee G, Yao J. Human tau filaments induce microtubule and synapse loss in an in vivo model of neurofibrillary degenerative disease. J Cell Sci. 2000; 113(Pt 8):1373–1387. [PubMed: 10725221]

He Y, Yu W, Baas PW. Microtubule reconfiguration during axonal retraction induced by nitric oxide. The Journal of neuroscience: the official journal of the Society for Neuroscience. 2002; 22:5982–5991. [PubMed: 12122060]

Hosie KA, King AE, Blizzard CA, Vickers JC, Dickson TC. Chronic excitotoxin-induced axon degeneration in a compartmented neuronal culture model. ASN Neuro. 2012; 4

Ichiyama T, Takahashi Y, Matsushige T, Kajimoto M, Fukunaga S, Furukawa S. Serum matrix metalloproteinase-9 and tissue inhibitor of metalloproteinase-1 levels in non-herpetic acute limbic encephalitis. J Neurol. 2009; 256:1846–1850. [PubMed: 19672673]

Irwin DJ, Cohen TJ, Grossman M, Arnold SE, Xie SX, Lee VM, Trojanowski JQ. Acetylated tau, a novel pathological signature in Alzheimer's disease and other tauopathies. Brain. 2012; 135:807–818. [PubMed: 22366796]

Ittner LM, Ke YD, Delerue F, Bi M, Gladbach A, van Eersel J, Wolfing H, Chieng BC, Christie MJ, Napier IA, Eckert A, Staufenbiel M, Hardeman E, Gotz J. Dendritic function of tau mediates amyloid-beta toxicity in Alzheimer's disease mouse models. Cell. 2010; 142:387–397. [PubMed: 20655099]

Johnson VE, Stewart W, Smith DH. Axonal pathology in traumatic brain injury. Exp Neurol. 2013; 246:35–43. [PubMed: 22285252]

Kaufman AC, Salazar SV, Haas LT, Yang J, Kostylev MA, Jeng AT, Robinson SA, Gunther EC, van Dyck CH, Nygaard HB, Strittmatter SM. Fyn inhibition rescues established memory and synapse loss in Alzheimer mice. Annals of neurology. 2015; 77:953–971. [PubMed: 25707991]

Kawaguchi Y, Kovacs JJ, McLaurin A, Vance JM, Ito A, Yao TP. The deacetylase HDAC6 regulates aggresome formation and cell viability in response to misfolded protein stress. Cell. 2003; 115:727–738. [PubMed: 14675537]

Khatoon S, Grundke-Iqbal I, Iqbal K. Brain levels of microtubule-associated protein tau are elevated in Alzheimer's disease: a radioimmuno-slot-blot assay for nanograms of the protein. Journal of neurochemistry. 1992; 59:750–753. [PubMed: 1629745]

Kilinc D, Gallo G, Barbee KA. Mechanical membrane injury induces axonal beading through localized activation of calpain. Exp Neurol. 2009; 219:553–561. [PubMed: 19619536]

Kim JY, Shen S, Dietz K, He Y, Howell O, Reynolds R, Casaccia P. HDAC1 nuclear export induced by pathological conditions is essential for the onset of axonal damage. Nature neuroscience. 2010; 13:180–189. [PubMed: 20037577]

Kurbatskaya K, Phillips EC, Croft CL, Dentoni G, Hughes MM, Wade MA, Al-Sarraj S, Troakes C, O'Neill MJ, Perez-Nievas BG, Hanger DP, Noble W. Upregulation of calpain activity precedes tau phosphorylation and loss of synaptic proteins in Alzheimer's disease brain. Acta Neuropathol Commun. 2016; 4:34. [PubMed: 27036949]

Lasagna-Reeves CA, Castillo-Carranza DL, Sengupta U, Sarmiento J, Troncoso J, Jackson GR, Kayed R. Identification of oligomers at early stages of tau aggregation in Alzheimer's disease. FASEB J. 2012; 26:1946–1959. [PubMed: 22253473]

Liang Z, Liu F, Iqbal K, Grundke-Iqbal I, Gong CX. Dysregulation of tau phosphorylation in mouse brain during excitotoxic damage. Journal of Alzheimer's disease: JAD. 2009; 17:531–539. [PubMed: 19363259]

LoPresti P, Konat GW. Hydrogen peroxide induces transient dephosphorylation of tau protein in cultured rat oligodendrocytes. Neurosci Lett. 2001; 311:142–144. [PubMed: 11567798]

Maas T, Eidenmuller J, Brandt R. Interaction of tau with the neural membrane cortex is regulated by phosphorylation at sites that are modified in paired helical filaments. The Journal of biological chemistry. 2000; 275:15733–15740. [PubMed: 10747907]

Meeker RB, Poulton W, Clary G, Schriver M, Longo FM. Novel p75 neurotrophin receptor ligand stabilizes neuronal calcium, preserves mitochondrial movement and protects against HIV associated neuropathogenesis. Exp Neurol. 2016; 275(Pt 1):182–198. [PubMed: 26424436]

Michaluk P, Mikasova L, Groc L, Frischknecht R, Choquet D, Kaczmarek L. Matrix metalloproteinase-9 controls NMDA receptor surface diffusion through integrin beta1 signaling. The Journal of neuroscience: the official journal of the Society for Neuroscience. 2009; 29:6007–6012. [PubMed: 19420267]

Min SW, Chen X, Tracy TE, Li Y, Zhou Y, Wang C, Shirakawa K, Minami SS, Defensor E, Mok SA, Sohn PD, Schilling B, Cong X, Ellerby L, Gibson BW, Johnson J, Krogan N, Shamloo M, Gestwicki J, Masliah E, Verdin E, Gan L. Critical role of acetylation in tau-mediated neurodegeneration and cognitive deficits. Nat Med. 2015; 21:1154–1162. [PubMed: 26390242]

Morris M, Knudsen GM, Maeda S, Trinidad JC, Ioanoviciu A, Burlingame AL, Mucke L. Tau post-translational modifications in wild-type and human amyloid precursor protein transgenic mice. Nature neuroscience. 2015; 18:1183–1189. [PubMed: 26192747]

Mroczko B, Groblewska M, Barcikowska M. The role of matrix metalloproteinases and tissue inhibitors of metalloproteinases in the pathophysiology of neurodegeneration: a literature study. Journal of Alzheimer's disease: JAD. 2013; 37:273–283. [PubMed: 23792694]

Nubling G, Levin J, Bader B, Israel L, Botzel K, Lorenzl S, Giese A. Limited cleavage of tau with matrix-metalloproteinase MMP-9, but not MMP-3, enhances tau oligomer formation. Exp Neurol. 2012; 237:470–476. [PubMed: 22890115]

Okamoto K, Hirai S, Shoji M, Senoh Y, Yamazaki T. Axonal swellings in the corticospinal tracts in amyotrophic lateral sclerosis. Acta Neuropathol. 1990; 80:222–226. [PubMed: 2202191]

Perez M, Santa-Maria I, Gomez de Barreda E, Zhu X, Cuadros R, Cabrero JR, Sanchez-Madrid F, Dawson HN, Vitek MP, Perry G, Smith MA, Avila J. Tau--an inhibitor of deacetylase HDAC6 function. Journal of neurochemistry. 2009; 109:1756–1766. [PubMed: 19457097]

Pike CJ, Cummings BJ, Cotman CW. beta-Amyloid induces neuritic dystrophy in vitro: similarities with Alzheimer pathology. NeuroReport. 1992; 3:769–772. [PubMed: 1421135]

Pooler AM, Usardi A, Evans CJ, Philpott KL, Noble W, Hanger DP. Dynamic association of tau with neuronal membranes is regulated by phosphorylation. Neurobiol Aging. 2012; 33:431e427–438.

Qin L, Wu X, Block ML, Liu Y, Breese GR, Hong JS, Knapp DJ, Crews FT. Systemic LPS causes chronic neuroinflammation and progressive neurodegeneration. Glia. 2007; 55:453–462. [PubMed: 17203472]

Roberson ED, Halabisky B, Yoo JW, Yao J, Chin J, Yan F, Wu T, Hamto P, Devidze N, Yu GQ, Palop JJ, Noebels JL, Mucke L. Amyloid-beta/Fyn-induced synaptic, network, and cognitive impairments depend on tau levels in multiple mouse models of Alzheimer's disease. The Journal of neuroscience: the official journal of the Society for Neuroscience. 2011; 31:700–711. [PubMed: 21228179]

Roberson ED, Scearce-Levie K, Palop JJ, Yan F, Cheng IH, Wu T, Gerstein H, Yu GQ, Mucke L. Reducing endogenous tau ameliorates amyloid beta-induced deficits in an Alzheimer's disease mouse model. Science. 2007; 316:750–754. [PubMed: 17478722]

Roediger B, Armati PJ. Oxidative stress induces axonal beading in cultured human brain tissue. Neurobiol Dis. 2003; 13:222–229. [PubMed: 12901836]

Rozkalne A, Hyman BT, Spires-Jones TL. Calcineurin inhibition with FK506 ameliorates dendritic spine density deficits in plaque-bearing Alzheimer model mice. Neurobiol Dis. 2011; 41:650–654. [PubMed: 21134458]

Sanchez-Varo R, Trujillo-Estrada L, Sanchez-Mejias E, Torres M, Baglietto-Vargas D, Moreno-Gonzalez I, De Castro V, Jimenez S, Ruano D, Vizuete M, Davila JC, Garcia-Verdugo JM, Jimenez AJ, Vitorica J, Gutierrez A. Abnormal accumulation of autophagic vesicles correlates with axonal and synaptic pathology in young Alzheimer's mice hippocampus. Acta Neuropathologica. 2012; 123:53–70. [PubMed: 22020633]

Schwalbe M, Biernat J, Bibow S, Ozenne V, Jensen MR, Kadavath H, Blackledge M, Mandelkow E, Zweckstetter M. Phosphorylation of human Tau protein by microtubule affinity-regulating kinase 2. Biochemistry. 2013; 52:9068–9079. [PubMed: 24251416]

Scott BA, Avidan MS, Crowder CM. Regulation of hypoxic death in C. elegans by the insulin/IGF receptor homolog DAF-2. Science. 2002; 296:2388–2391. [PubMed: 12065745]

Selenica ML, Benner L, Housley SB, Manchec B, Lee DC, Nash KR, Kalin J, Bergman JA, Kozikowski A, Gordon MN, Morgan D. Histone deacetylase 6 inhibition improves memory and reduces total tau levels in a mouse model of tau deposition. Alzheimer's research & therapy. 2014; 6:12.

Stokin GB, Lillo C, Falzone TL, Brusch RG, Rockenstein E, Mount SL, Raman R, Davies P, Masliah E, Williams DS, Goldstein LS. Axonopathy and transport deficits early in the pathogenesis of Alzheimer's disease. Science. 2005; 307:1282–1288. [PubMed: 15731448]

Stomrud E, Bjorkqvist M, Janciauskiene S, Minthon L, Hansson O. Alterations of matrix metalloproteinases in the healthy elderly with increased risk of prodromal Alzheimer's disease. Alzheimer's research & therapy. 2010; 2:20.

Tagliaferro P, Burke RE. Retrograde Axonal Degeneration in Parkinson Disease. J Parkinsons Dis. 2016; 6:1–15.

Takeuchi H, Mizuno T, Zhang G, Wang J, Kawanokuchi J, Kuno R, Suzumura A. Neuritic beading induced by activated microglia is an early feature of neuronal dysfunction toward neuronal death by inhibition of mitochondrial respiration and axonal transport. JBiolChem. 2005; 280:10444–10454.

Takeuchi H, Mizuno T, Zhang G, Wang J, Kawanokuchi J, Kuno R, Suzumura A. Neuritic beading induced by activated microglia is an early feature of neuronal dysfunction toward neuronal death by inhibition of mitochondrial respiration and axonal transport. The Journal of biological chemistry. 2005; 280:10444–10454. [PubMed: 15640150]

Tan Z, Sun X, Hou FS, Oh HW, Hilgenberg LG, Hol EM, van Leeuwen FW, Smith MA, O'Dowd DK, Schreiber SS. Mutant ubiquitin found in Alzheimer's disease causes neuritic beading of mitochondria in association with neuronal degeneration. Cell Death Differ. 2007; 14:1721–1732. [PubMed: 17571083]

Tracy TE, Sohn PD, Minami SS, Wang C, Min SW, Li Y, Zhou Y, Le D, Lo I, Ponnusamy R, Cong X, Schilling B, Ellerby LM, Huganir RL, Gan L. Acetylated Tau Obstructs KIBRA-Mediated Signaling in Synaptic Plasticity and Promotes Tauopathy-Related Memory Loss. Neuron. 2016; 90:245–260. [PubMed: 27041503]

Verdel A, Curtet S, Brocard MP, Rousseaux S, Lemercier C, Yoshida M, Khochbin S. Active maintenance of mHDA2/mHDAC6 histone-deacetylase in the cytoplasm. Curr Biol. 2000; 10:747–749. [PubMed: 10873806]

Wilczynski GM, Konopacki FA, Wilczek E, Lasiecka Z, Gorlewicz A, Michaluk P, Wawrzyniak M, Malinowska M, Okulski P, Kolodziej LR, Konopka W, Duniec K, Mioduszewska B, Nikolaev E, Walczak A, Owczarek D, Gorecki DC, Zuschratter W, Ottersen OP, Kaczmarek L. Important role of matrix metalloproteinase 9 in epileptogenesis. The Journal of cell biology. 2008; 180:1021–1035. [PubMed: 18332222]

Williams KS, Killebrew DA, Clary GP, Seawell JA, Meeker RB. Differential regulation of macrophage phenotype by mature and pro-nerve growth factor. J Neuroimmunol. 2015; 285:76–93. [PubMed: 26198923]

Xiao AW, He J, Wang Q, Luo Y, Sun Y, Zhou YP, Guan Y, Lucassen PJ, Dai JP. The origin and development of plaques and phosphorylated tau are associated with axonopathy in Alzheimer's disease. Neurosci Bull. 2011; 27:287–299. [PubMed: 21934724]

Yan J. Interplay between HDAC6 and its interacting partners: essential roles in the aggresome-autophagy pathway and neurodegenerative diseases. DNA Cell Biol. 2014; 33:567–580. [PubMed: 24932665]

Zempel H, Thies E, Mandelkow E, Mandelkow EM. Abeta oligomers cause localized Ca(2+) elevation, missorting of endogenous Tau into dendrites, Tau phosphorylation, and destruction of microtubules and spines. The Journal of neuroscience: the official journal of the Society for Neuroscience. 2010; 30:11938–11950. [PubMed: 20826658]

Zhang L, Liu C, Wu J, Tao JJ, Sui XL, Yao ZG, Xu YF, Huang L, Zhu H, Sheng SL, Qin C. Tubastatin A/ACY-1215 improves cognition in Alzheimer's disease transgenic mice. Journal of Alzheimer's disease: JAD. 2014; 41:1193–1205. [PubMed: 24844691]

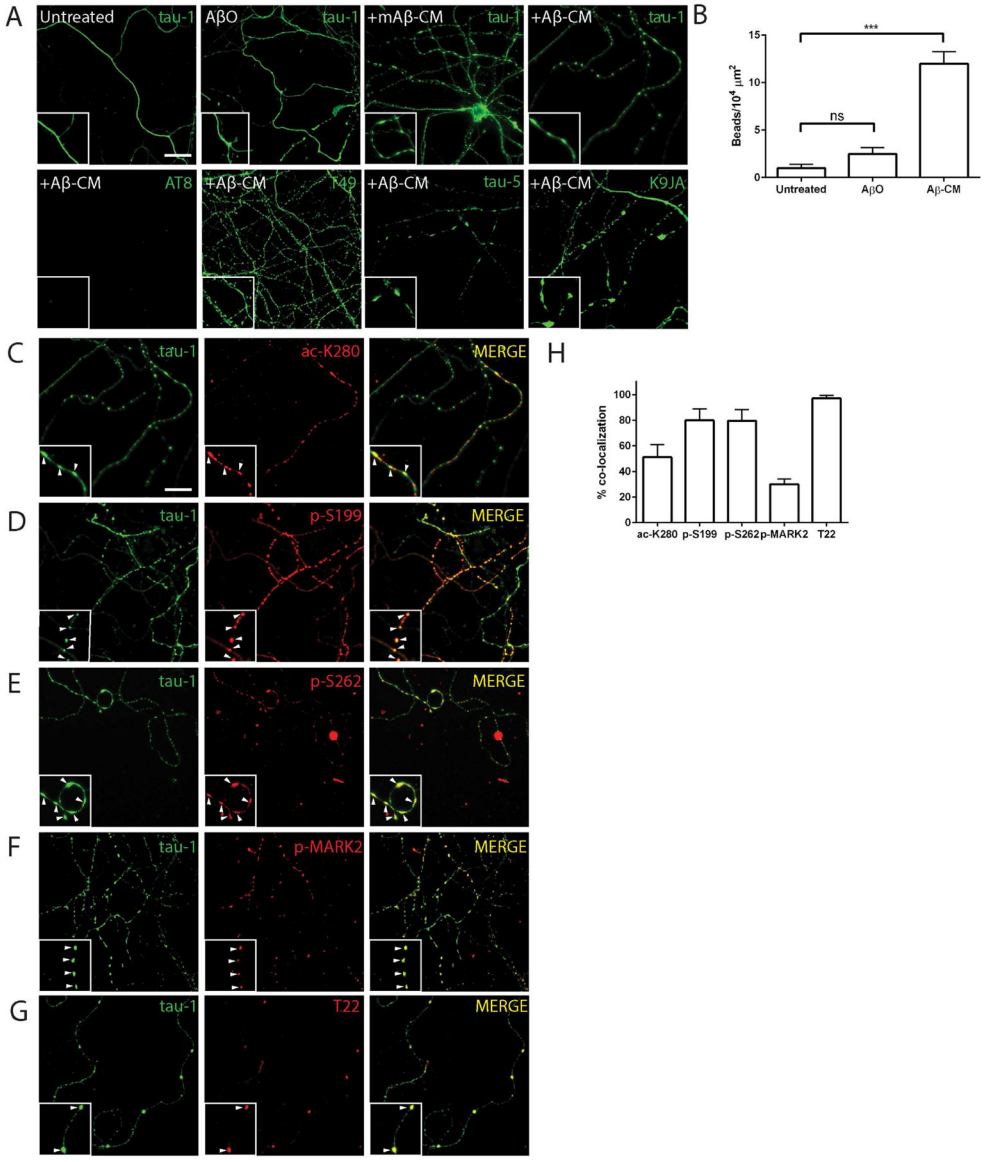

Figure 1. Aβ-oligomer induced secretion of neuroinflammatory factors promotes endogenous neuritic tau beading in primary neurons

(A) Primary cortical neurons were exposed to Aβ oligomers (AβO, 1 μM) or a 1:4 dilution of microglia-derived (mAβ-CM) or hMDM-derived (Aβ-CM) conditioned media for 5 h followed by fluorescent microscopy analysis using the dephosphorylation-specific tau-1 antibody, phospho-tau AT8 antibody, or total mouse tau antibodies T49, tau-5, and K9JA (green). Scale bar = 50 μm.

(B) Quantification of beads formed per 10^4 μm^2 indicated hMDM-derived Aβ-CM increased neuritic tau bead formation, while direct addition of AβO alone did not significantly alter bead formation. Error bars indicate S.E.M (***, p-value < 0.001).

(C–H) Primary cortical neurons were treated with Aβ-CM at a 1:4 dilution for 5 h and were analyzed by double-labeling with tau-1 antibody (green) in combination with ac-K280 (C), pS199 (D), pS262 (E), pMARK2 (F), or tau T22 oligomer antibodies (G) (red). Co-

localization of tau-1 immunoreactive foci with the indicated antibodies is highlighted by arrowheads in the inset.

(H) Quantification of co-localization was determined as percent of tau-1 co-localization per total number of tau-1-positive foci. Error bars indicate S.E.M.

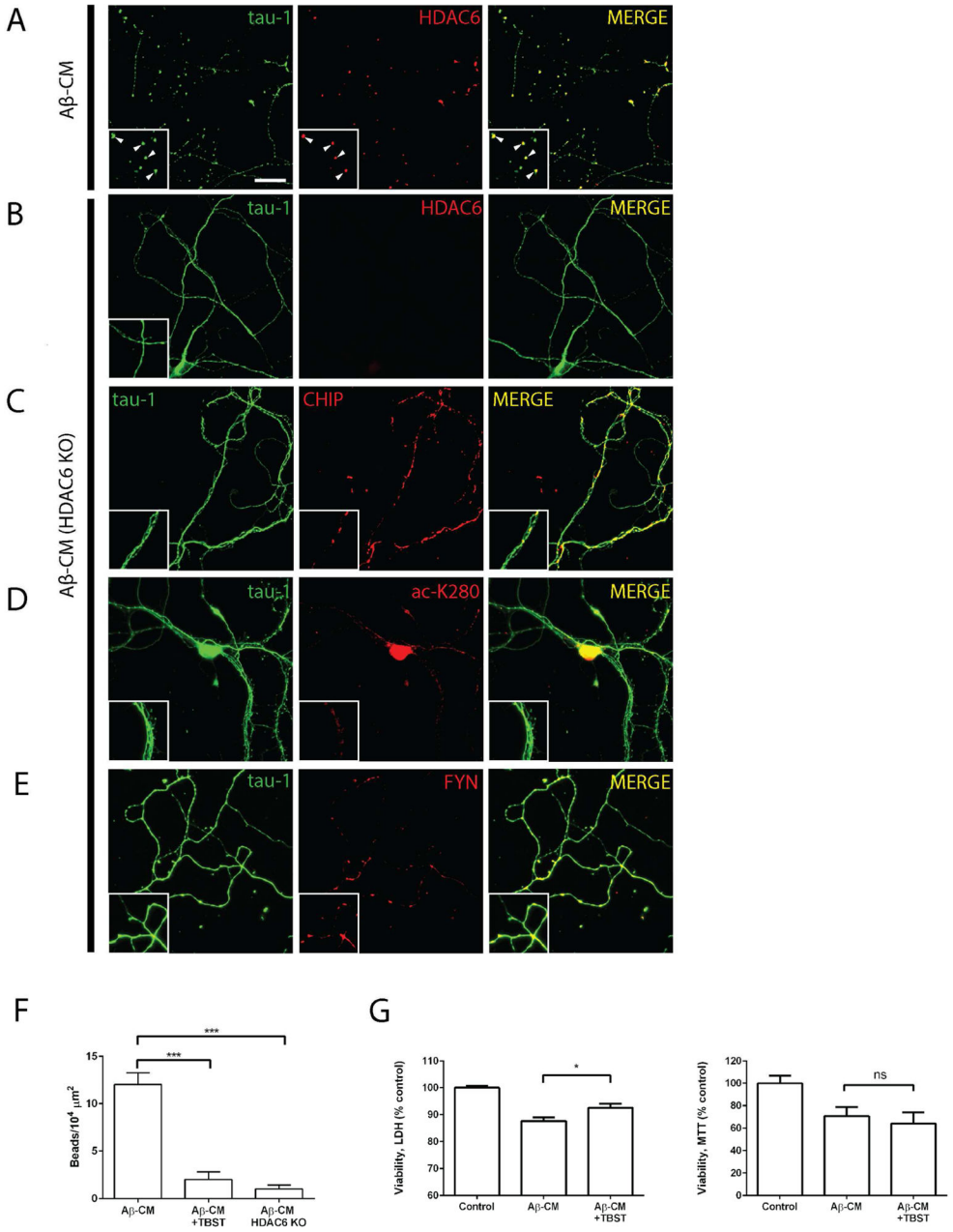

Figure 2. Depletion or inhibition of the deacetylase HDAC6 suppresses endogenous neuritic tau beading

(A–E) Wild-type or HDAC6 KO cortical neurons treated with Aβ-CM were double-labeled with tau-1 (green) in combination with HDAC6 (A, B), ac-K280 (C), CHIP (D) or FYN (E) (red). Scale bar = 50 μm.

(F) Quantification of beads formed per 10^4 μm^2 indicated significantly decreased neuritic bead formation in HDAC6 KO neurons and TBST-treated wild-type neurons (see also Figure S5).

(G) Neuronal viability assays (LDH, MTT assays) were performed on primary cortical neurons treated with Aβ-CM in the absence or presence of TBST, which alleviated

neurotoxicity by LDH assay but did not affect metabolic activity detected by the MTT assay. Error bars indicate S.E.M (ns = not significant; *, p-value < 0.05; ***, p-value < 0.001).

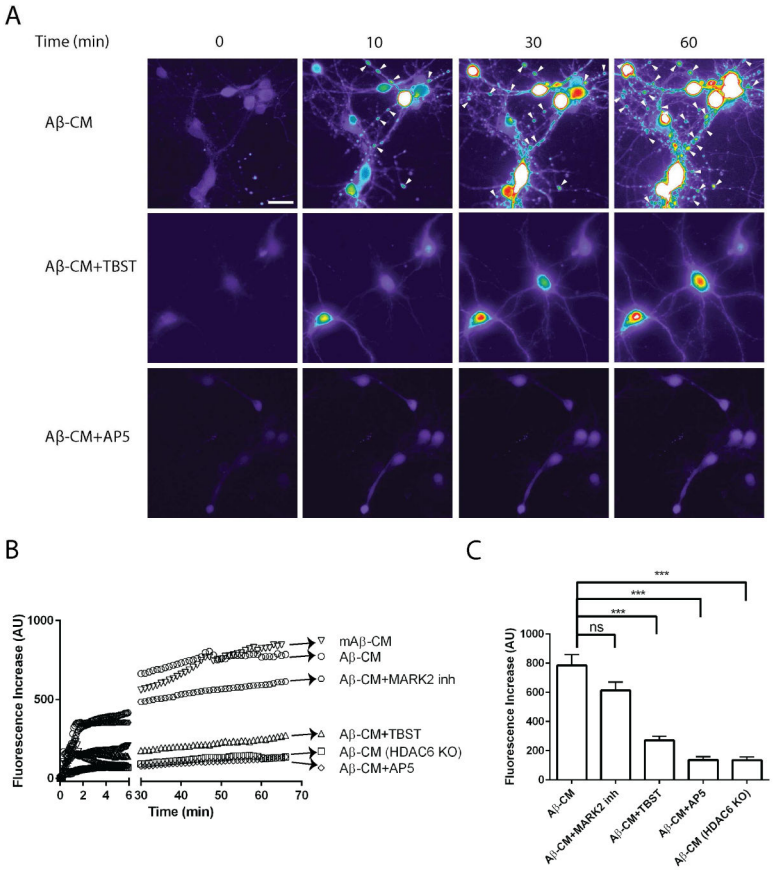

Figure 3. Aβ-oligomer induced neuroinflammatory stress promotes calcium dysfunction in an HDAC6-dependent manner

(A) Live calcium imaging using the calcium indicator Fluo-4 AM was performed on primary cortical neurons challenged with Aβ-CM in the absence or presence of TBST or the NR antagonist AP5. Scale bar = 50 μm.

(B) Exposure to Aβ-CM or mAβ-CM promoted gradual intracellular calcium increases (as detected by fluorescence intensity) that was potently suppressed by loss or inhibition of HDAC6 (HDAC6 KO or TBST) or by pre-treatment with the NR inhibitor AP5.

(C) The final delayed phase calcium increase is shown in wild-type or HDAC6 KO neurons pre-treated with MARK inhibitor 39621, TBST or AP5 (***, p-value < 0.001).

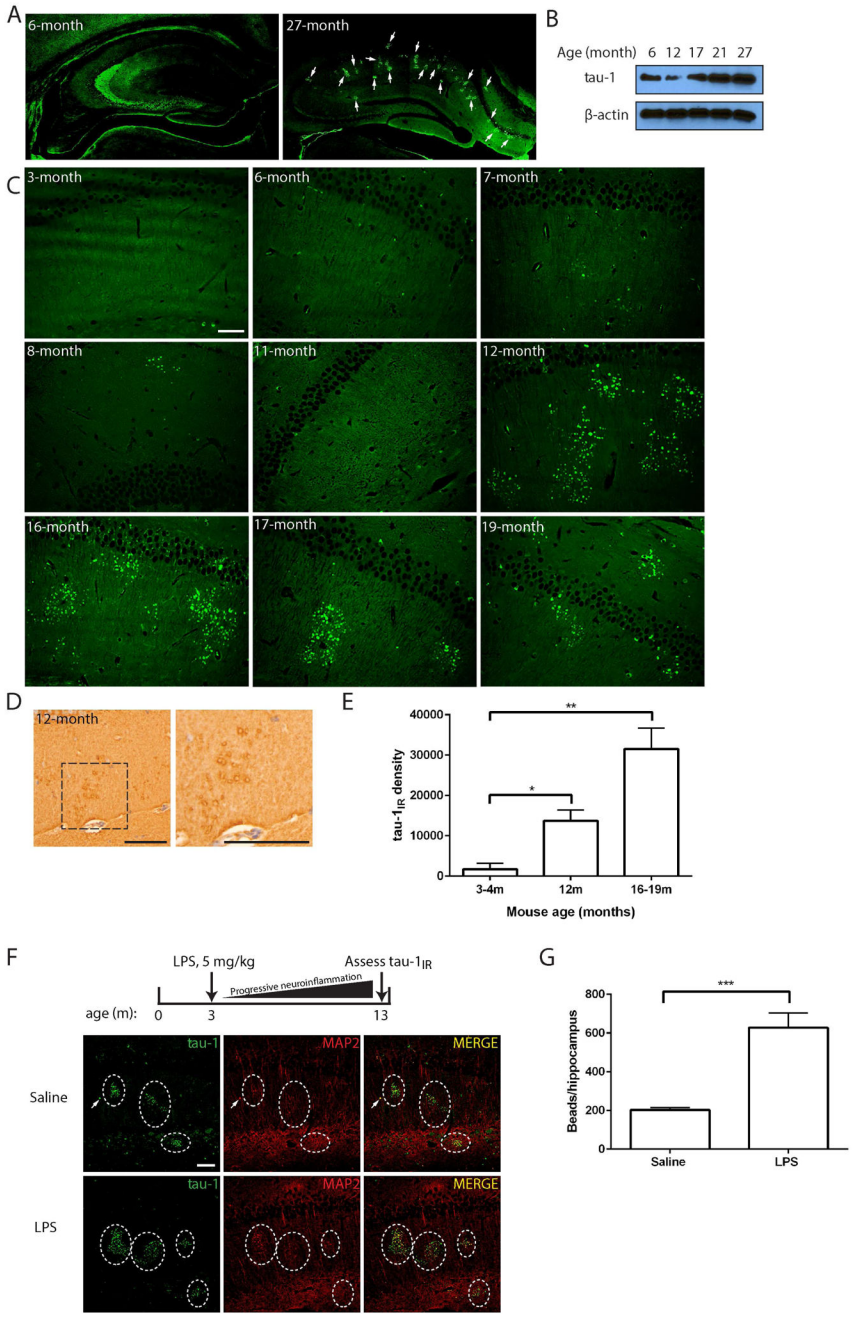

Figure 4. Neuritic tau-1_{IR} clusters accumulate *in vivo* during aging or neuroinflammatory stress

(A) Young (6-month) or old (27-month) wild type mouse brains were analyzed by confocal microscopy using the tau-1 antibody (green). The full hippocampus is depicted. Aged mice showed large tau-1-positive aggregates and clusters throughout the CA1 and other hippocampal regions as well as select cortical brain regions.

(B) Immunoblotting analysis of mouse hippocampal homogenates depicting tau-1 immunoreactivity in young and aged mice.

(C–D) CA1 regions of aged wild type mice from 3 to 19 months old were analyzed by confocal microscopy or immunohistochemistry (D) to detect tau-1_{IR} pathology. Tau-1_{IR} foci

(green) started to accumulate in the hippocampus after 6 months. By 12 months, more detectable and widespread tau-1_{IR} pathology was observed. Scale bar, 50 μm.
(E) Tau-1_{IR} clusters were quantified in young vs. old mice. Error bars indicate S.E.M. ns = not significant; *, p-value < 0.05; **, p-value < 0.01. Scale bar = 100 μm.
(F–G) Saline control or LPS injected 3 month old wild-type mice were analyzed 10 months post injection and tau-1_{IR} clusters in the hippocampus were quantified (G). Scale bar = 50 μm.

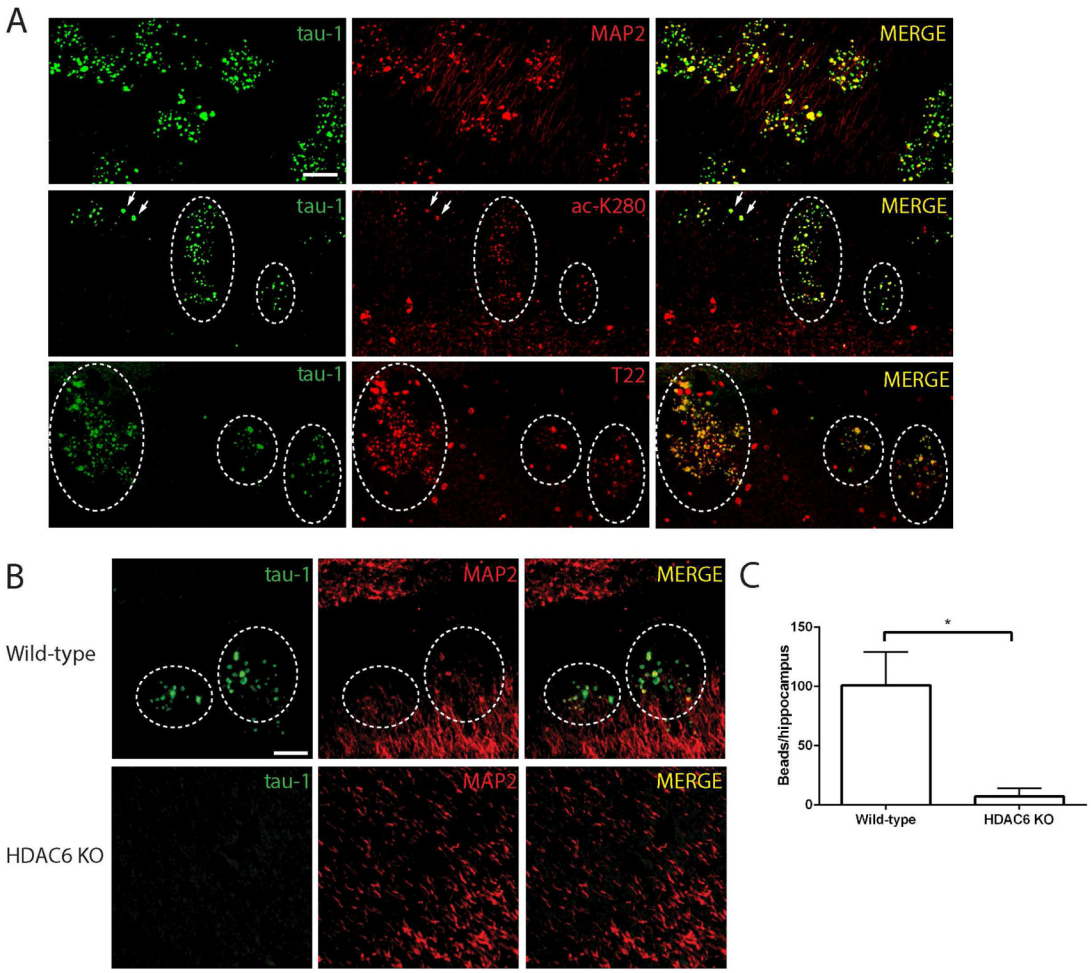

Figure 5. Acetylated oligomeric tau-1_{IR} clusters develop in aged wild-type mice and are reduced in HDAC6 KO mice

(A) Aged wild-type mouse brains were double-labeled with tau-1 (green) in combination with MAP2, ac-K280, or T22 antibodies (red) and hippocampal regions were imaged by confocal microscopy. Prominent regions of co-localization are highlighted by arrowheads (depicting large single aggregates) and multi-aggregated tau-1_{IR} clusters are highlighted within the dashed white circles. Scale bar = 50 μm.

(B) WT and HDAC6 KO mice (12 month old) were analyzed by double-labeling immunofluorescence to detect tau-1_{IR} pathology (green) as well as dendritic tau mislocalization (MAP2, red) in the hippocampus. Scale bar = 50 μm

(C) Quantification of tau-1_{IR} beads per hippocampus was determined from WT and HDAC6 KO mice (n=5 mice for each genotype; *, p-value < 0.05).

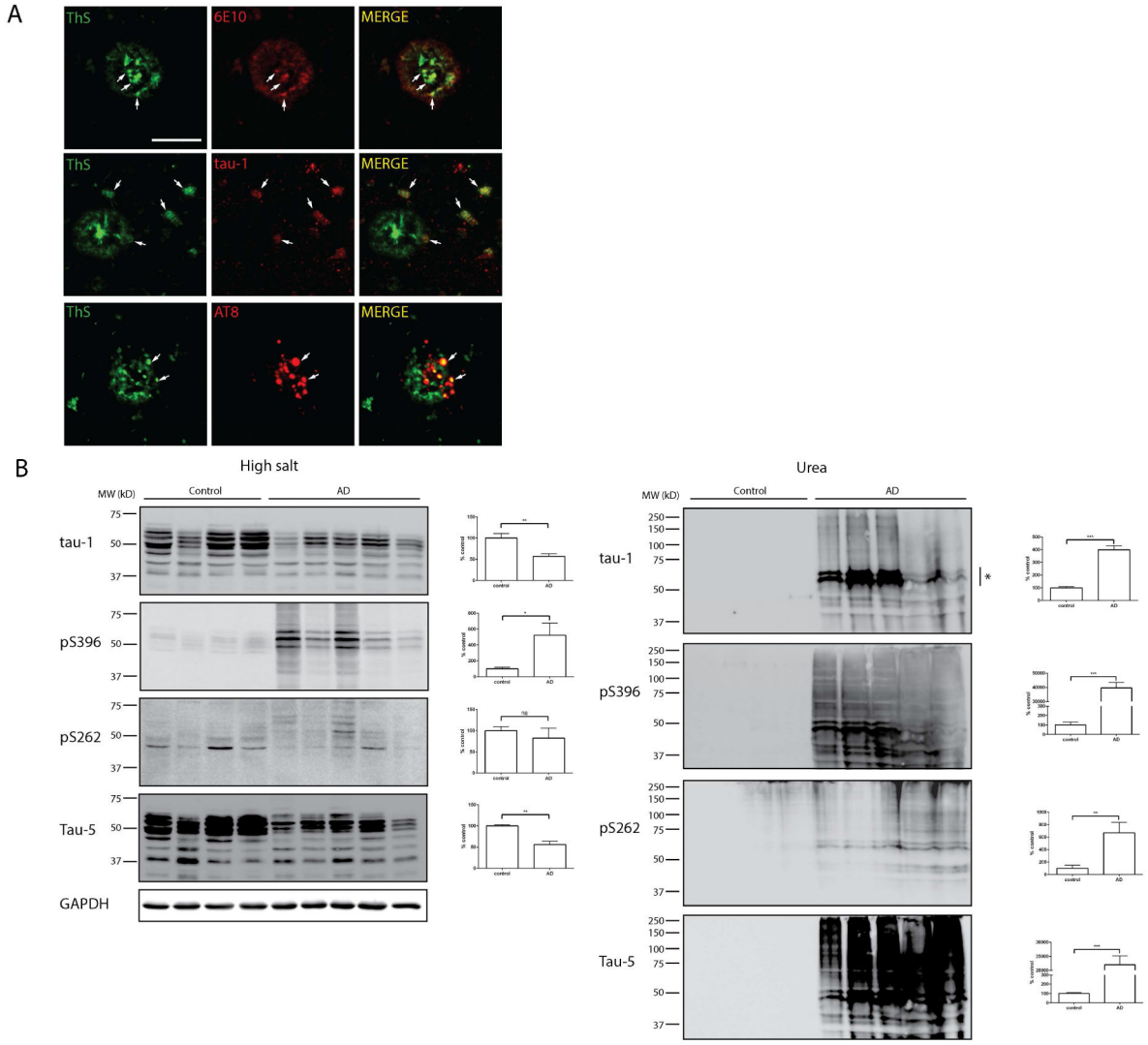

Figure 6. Dephosphorylated tau-1$_{IR}$ pathology is detected in human AD brain

(A) Cortical brain sections from human AD patients were analyzed by double-labeling using tau-1, AT8, or 6E10 antibodies along with Thioflavin S (ThS) to label AD pathology. The double-labeling illustrates tau-1$_{IR}$ immunoreactivity associated with ThS (white arrows). Scale bar = 50 μm.

(B) Biochemical fractionation of frontal cortex gray matter was performed and analyzed by immunoblotting using the indicated tau antibodies. Tau immunoreactivity was quantified from soluble (high-salt extracted) and insoluble (urea extracted) fractions using ImageQuant v8.1 and differences are represented as fold change compared to control non-AD samples. ns = not significant; *, p-value < 0.05; **, p-value < 0.01.

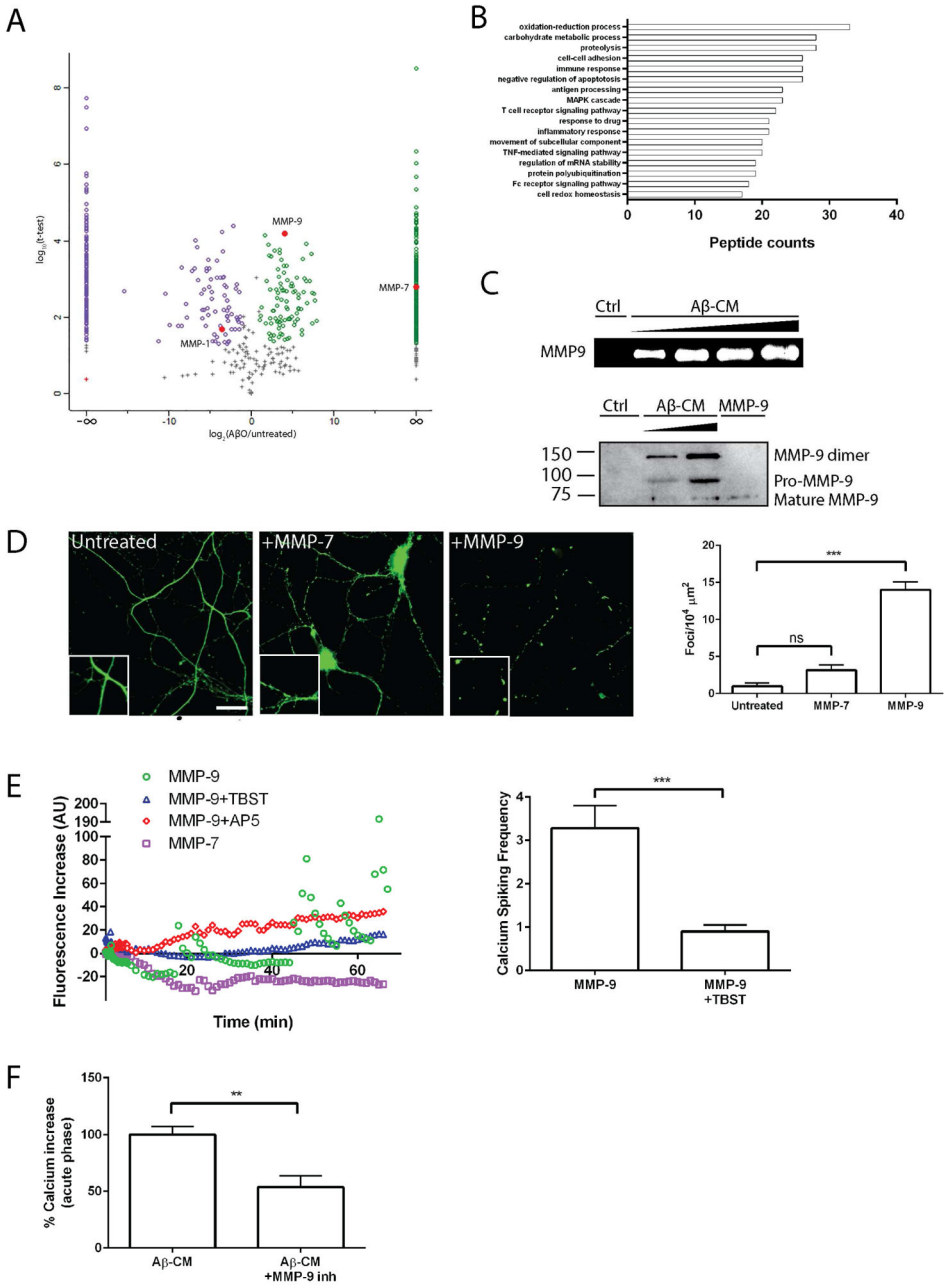

Figure 7. Mass spectrometry profiling of the Aβ-oligomer induced secretome identified MMP-9 as a regulator of neuritic tau beading

(A) A volcano plot of LC-MS/MS data generated from the secretome analysis of untreated or Aβ oligomer-treated hMDM. Relative protein abundance was plotted on the x-axis as $\log_2$ ratios. Negative $\log_{10}$ transformed p-values were plotted on the y-axis. Significant protein hits (p-value < 0.05) are represented by green (up-regulated) and blue circles (down-regulated). MMP-1, -7 and -9 were significantly altered, as indicated by red circles in the volcano plot. The proteins on the far left and right sides were only identified in either untreated (left) or Aβ oligomer-treated hMDM (right).

(B) Top protein biological processing categories obtained with the **D**atabase for **A**nnotation, **V**isualization and **I**ntegrated **D**iscovery (**DAVID**) are highlighted from Aβ oligomer-induced secretome.

(C) Zymography analysis and immunoblotting showed the presence of secreted and active MMP-9 in Aβ-CM.

(D) Primary cortical neurons treated with MMP-7 or MMP-9 overnight were analyzed by confocal microscopy with the tau-1 antibody (green) revealing MMP-9-mediated neuritic bead formation. Scale bar = 50 μm.

(E) Live calcium imaging of primary cortical neurons challenged with purified recombinant MMP-7 or MMP-9 in the absence or presence of TBST or AP5. MMP-9 treatment resulted in distinct calcium spiking intensities in a subset of neurons that was suppressed by TBST. Calcium spiking frequency was quantified as total calcium spikes and is reported as spiking per 100 frames. Error bars indicate S.E.M.

(F) Aβ-CM was pre-incubated with an MMP-9 specific inhibitor prior to addition to neurons for subsequent live calcium imaging. The acute calcium rise in response to Aβ-CM was significantly suppressed by MMP-9 inhibition alone (**, p-value < 0.01; ***, p-value < 0.001).